Additive manufacture of superduplex stainless steel using WAAM

Magnus Eriksson[*, 1], *Malin* Lervåg[2], *Camilla* Sørensen[2], *Andreas* Robertstad[2], *Bård* M. Brønstad[2], *Bård* Nyhus[1], *Ragnhild* Aune[1], *Xiaobo* Ren[1] and *Odd M.* Akselsen[1, 2]

[1] SINTEF Industry, Trondheim, Norway
[2] NTNU, Dept. Mechanical and Industrial Engineering, Trondheim, Norway

Abstract. Superduplex stainless steels have been used in the oil and gas industry for a couple of decades due to the combination of excellent mechanical properties and corrosion resistance. The present investigation addresses the applicability of wire and arc additive manufacturing for this steel grade. Due to the inherent rapid heating and cooling, the initial base metal microstructure will be substantially altered, and complex thermal cycles may cause the formation of brittle secondary phases, among which the frequently observed intermetallic sigma phase is most harmful. However, no intermetallic phases have been observed, which is consistent with the low heat input employed, and the high Ni content in the wire. The microstructure observations in terms of ferrite volume fraction, Cr nitrides precipitation and the formation of secondary austenite are discussed together with the hardness measurements, tensile testing and notch toughness testing. It is concluded that additive manufacturing of superduplex stainless steels by wire and arc process is feasible.

1 Introduction

Significant progress in additive manufacturing (AM) technologies, commonly known as 3D printing, has taken place over the past decade. AM is a layer by layer manufacturing process. A single layer of metal is deposited upon a previous layer resulting in a complex, time dependent temperature profiles within the part being fabricated. The result is that the alloy may experience repeated solid state and liquid-solid phase transformations. The competitive position of AM for metal components relative to alternative manufacturing processes is a function of the geometrical complexity and production volume. While powder bed fusion AM is suitable to fabricate parts with medium to high geometrical complexity at relatively low quantities, the wire and arc additive manufacturing (WAAM) is more suitable for low to medium complexity. Up to date, there have been only a limited number of commercial alloys used in AM [1]. AM system may be classified/categorized in terms of the material feed stock, energy source, build volume, etc. As the AM field matures, new alloys will need to be developed to exploit the advantages of AM. Ti-6Al-4V

* Corresponding author: magnus.eriksson@sintef.no

has been by far the most extensively investigated. This can be attributed to the strong business case that can be developed for complex, low production volume titanium parts.

For metals, AM technologies are mainly classified into powder bead fusion, directed energy deposition, binder jetting and sheet lamination (ASTM F2792). Typical additive materials are metal powder and metal wire. The majorities of the research in AM have been focused on the powder-feed/-bed AM, where the laser or electron beam equipment is usually used as the power source [2]. The application of wire arc additive manufacturing (WAAM), often referred to as direct energy or direct metal deposition (DED or DMD), may promote the use AM technology since it is a relatively cheap and quick process, and most industry will have easily access to an arc welding infrastructure. During fabrication, a heat source (welding arc, electronic beam or laser) is moved along a path defined by the computer-aided design file of the component to be produced, melting individual particles of powder or wire to form the component. In the present study, the cold metal transfer (CMT) process was selected, based on controlled dip transfer mode mechanism providing high deposition rate and low heat input. CMT is a special, colder version of the conventional gas metal arc welding (GMAW) process.

As mentioned above, the most frequent studied metals in AM are Ti alloys. Although austenitic stainless steels such as AISI 304 and 316 have been subjected to AM [3-6], there is no result available for superduplex stainless steels (25Cr7Ni). Therefore, such steel was subjected to WAAM to study the effect of heat input on mechanical properties. In layer manufacturing of superduplex stainless steels, some concern about microstructure evolution may exist due to certain risk of intermetallics formation. High heat inputs with longer exposure to temperatures between 650 and 950 °C may cause precipitation of brittle intermetallic phases such as σ (sigma) or χ (chi), Cr_2N (chromium nitride) or γ_2 (secondary austenite). Of all these, σ phase formation is by far the most detrimental factor in terms of reducing ductility, toughness, and corrosion resistance, e.g., Ref. [7]. The ferrite formers Cr, Mo and Si are the main elements which increase the susceptibility to σ phase precipitation [8]. However, the heat inputs employed did not allow σ phase formation. On the other hand, it is shown that the fast cooling rates promoted precipitation of Cr nitrides.

2 Materials and experimental procedure

2.1 Materials

The materials employed in the present work were 1.2 mm superduplex steel wire with high Ni content (9.5%) and 0.6% W, and 12 mm thick support plate of 2507 superduplex steel. Their chemical composition is outlined in Table 1. The plate has yield and tensile strength of 662 and 834 MPa, respectively, for a ferrite volume fraction of 0.48.

Table 1. Chemical composition of selected welding wire (LNM Zeron 100X) and support plate.

Material	C	Si	Mn	P	S	Cr	Ni	Mo	Cu	N	W
Wire	0.018	0.3	0.7	0.02	0.001	25.0	9.5	3.7	0.6	0.23	0.6
Plate	0.020	0.32	0.85	0.023	0.0003	24.8	6.6	3.7	0.16	0.26	n.a.[1]

[1] n.a.: not added

2.2 Layer deposition

All beads were welded using a cold metal transfer (CMT) power source (Fronius TransPuls Synergic 3200 Pipe HE). CMT is a colder version of the conventional gas metal arc welding (GMAW) process. One of the advantages with this process is the absence of spatter, which is essential in additive manufacturing. The welding parameters employed are outlined in Table 2. The shielding gas was Mison® 2, consisting of Argon, 2% CO_2, and

0.03% NO, using a flow rate of 20 l/min. The average bead height for the three different walls was 2.4, 2.8 and 3.4 mm for welds 1-3, respectively, which is consistent with the heat input variation. The maximum interpass temperature was set to 100°C. The combined effect of heat input and interpass temperature on the weld cooling program may be of concern for superduplex stainless steels due to the risk of formation of brittle intermetallic phases like σ (sigma). Due to the low interpass, which was set because of the limited plate dimensions, there was a delay of 20-30 minutes between each layer for the highest heat input employed. In an industrial production, this is not required since the support plate (if used) dimensions will be larger. Prior to welding, the plate was cleaned with ethanol to remove dirt.

Table 2. Layer deposition parameters.

Parameter	Weld No		
	W2	W3	W1
Current (A)	185	212	212
Voltage (V)	14	14	14
Travel speed (mm/s)	6.4	5.5	3.4
Heat input (kJ/mm)	0.4	0.54	0.87
Wire feed rate (mm/s)	84.7	106	106
Polarity	DC+	DC+	DC+

2.3 Testing and characterization

The deposited walls were cut to carry out macroscopic inspection, tensile testing and metallographic evaluation of hardness and microstructures. For the tensile test, samples were extracted both parallel (horizontal) and perpendicular (vertical) to the layer deposition direction with dimensions of 12mm length, 4mm diameter and 4mm gauge length (L_0).

Three Charpy V notch subsized samples of 5 x 10 mm^2 cross section and 55 mm length were cut and machined with the length axis parallel with the welding direction. The notch was positioned with the fracture direction perpendicular to the welding direction. In addition, 6 Charpy V specimens were also taken from the base metal; 3 of them are subsized with the same dimensions as above, and 3 with full sized 10 x 10 mm^2 cross section. This was done to have refence toughness for comparison. The testing was subsequently carried out at -20°C. The absorbed energy of subsized specimens were multiplied by a factor of 2 for conversion to full size, in agreement with the DNV GL standard OS-F101 (2013). One cross section of the wall from each weld heat input was cut perpendicular to the layer length direction for macroscopic inspection, Vickers pyramid hardness measurements (HV_{10}, with 10 kg force) and microstructure characterization. These samples were subjected to standard metallographic techniques such as grinding and polishing, as well as etching for point counting of the ferrite content in the first and the last bead, as well as in the heat affected zone and base metal.

3 Results and discussion

3.1 Macroscopic inspection

The layer manufactured walls were measured to be of around 295 mm length, while the widths were 7.5, 8.5 and 11 mm for heat inputs of 0.4, 0.54 and 0.87 kJ/mm, respectively. The corresponding total number of beads were 12, 11 and 8. The beads are visible in Fig.1.

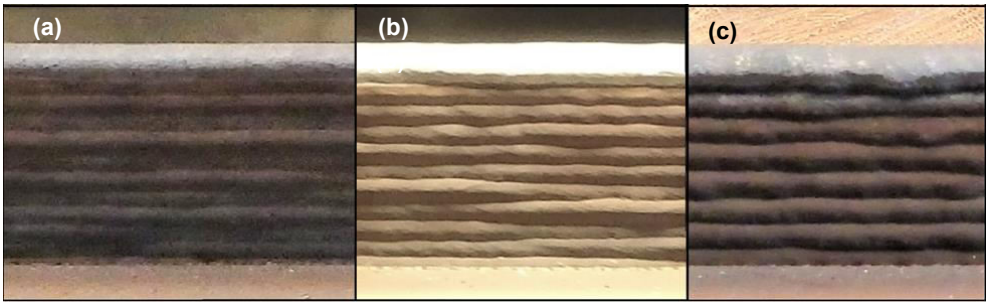

Fig.1. Deposited layers; (a) 0.4 kJ/mm, (b) 0.54 kJ/mm, and (c) 0.87 kJ/mm.

3.2 Tensile data

Both yield and tensile strength are reduced with increasing heat input as evidenced by the data plotted in Fig.2. The slope is larger for yield than for tensile strength. For the highest heat input, there is lower strength than for the base metal. By contrast to strength, the ductility increases with increasing heat input.

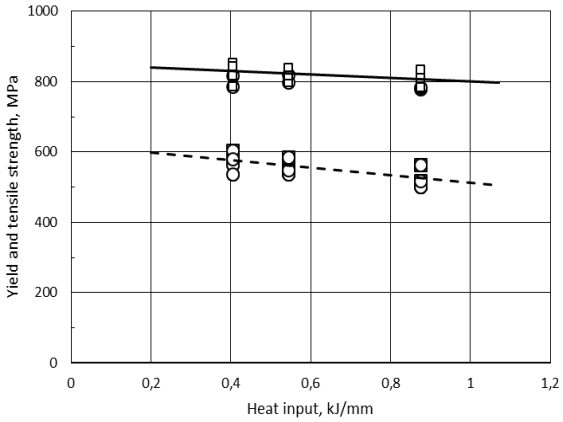

Fig.2. Effect of heat input on yield and tensile strength levels. Symbols: Vertical samples; • Horizontal samples.

3.3 Hardness

The results from hardness measurement are shown graphically in Fig.3. The highest hardness value is achieved in the heat affected zone (HAZ) with highest individual hardness of 271 kg/mm^2 for the lowest heat input. The hardness level of both the deposited layers and the HAZ are quite low and will thus satisfy maximum hardness requirements. The only requirement that is not met is the one set to sour service, usually 248 Vickers numbers (~ 22 Rockwell C). The maximum hardness in HAZ and WM can be reduced through an increase in heat input. Extrapolation in Fig.3 reveals that the 248 hardness in the HAZ requires a heat input of around 1 kJ/mm. However, the heat input cannot be increased uncritically since it is essential to avoid formation of unfavourable microstructures in HAZ. In the present case with superduplex steel wire, the HAZ and weld metal is expected to be more sensitive to σ and χ formation due to a higher ratio between ferrite (e.g., Cr, Mo, Si) and austenite (Ni, Mn, Cu, N) stabilizers.

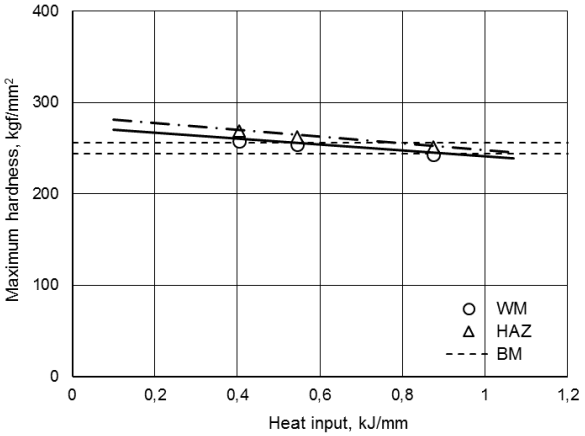

Fig.3. Effect of heat input on hardness of deposited layers.

3.4 Toughness

The notch toughness is plotted versus heat input in Fig.4. For comparison, the base metal data are plotted (two dotted lines), representing full Charpy samples and subsized specimens, converted to full size, i.e., multiplied by a factor of 2 to compensate for twice as large cross section. The converted value is very close to the values achieved for full size Charpy specimens.

It is seen from Fig.4 that the toughness of the wall is only one third of the initial base metal toughness. It is also seen that the toughness level is nearly independent of the heat input employed. This probably means that no harmful intermetallic phases have been formed (to be discussed later). However, the substantially lower toughness of the wall must be related to microstructures formed on cooling. It is likely that the toughness fall is linked to the grain coarsening taking place during the welding heat cycles, and the subsequent transformation to non-equilibrium coarse microstructures.

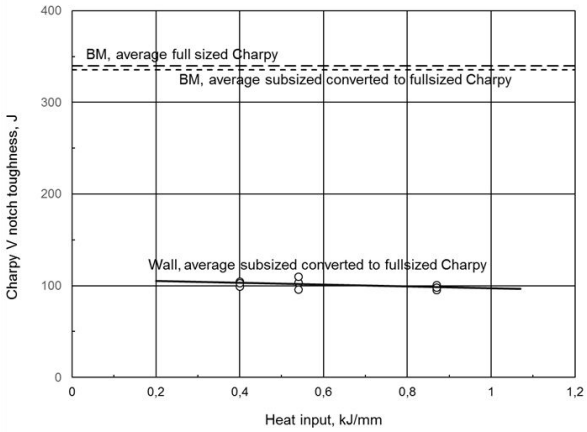

Fig.4. Charpy V notch toughness of walls. Base metal included for comparison (dotted lines).

3.4 Microstructures

The base metal consisted of ferrite (48 vol%) and austenite (52 vol%). In welding, the base metal austenite in the duplex (δ/γ) microstructure transforms to ferrite on heating. Further heating will induce grain growth of the transformed ferrite. During the cooling leg,

the high temperature ferrite phase may re-transform to austenite, depending on the cooling rate. Close to the fusion line on the HAZ side, the austenite to ferrite transformation proceeds to completion, leaving a ferritic microstructure at the end of heating. With lower peak temperatures, the transformation proceeds to only partial completion, resulting in a microstructure containing both transformed and untransformed austenite [9]. It is well known that the impact toughness of duplex stainless steel weldment may deteriorate with the increase in volume fraction of δ-ferrite within HAZ [10-12]. Localized uneven distribution of ferrite/austenite with 80–90% ferrite in weld is found [13]. The weldability of duplex stainless steels has been improved by the addition of nitrogen to stabilize the austenite at elevated temperatures [14], with an enhancement of mechanical and corrosion properties [15-19]. On the other hand, the re-precipitation of austenite from δ-ferrite is also enhanced due to a higher nitrogen content in modern duplex stainless steels [20].

In the case of superduplex stainless steels, it is evident from Fig.5 that the ferrite volume fraction varied depending on position, with much lower fraction in the deposited layers than in the base metal and HAZ with fractions between 15 and 27%. The fraction of ferrite is highest in the top layer, where there is no new reheating from subsequent beads. The low ferrite amount is caused by the welding wire which contains almost 3% higher nickel content than the base metal, i.e., 9.5 versus 6.6% Ni. In fact, weld filler materials are usually overalloyed with 2–4% more Ni than in the base material to restore the phase balance [21]. In addition to ferrite, both austenite stringers and Widmanstätten side-plate austenite have been found. The ferrite content was higher in HAZ, varying between 49 and 56%, which is slightly depending on the heat input. Due to the balanced alloying of superduplex stainless steels, the volume fraction of ferrite in the high temperature part of HAZ is rather low compared with that of conventional 2205 or 2304 duplex stainless steel. The microstructure shown in Fig.6a consists of large ferrite grains with allotriomorphic austenite along the grain boundaries and high volume fraction of Widmanstätten side-plate austenite.

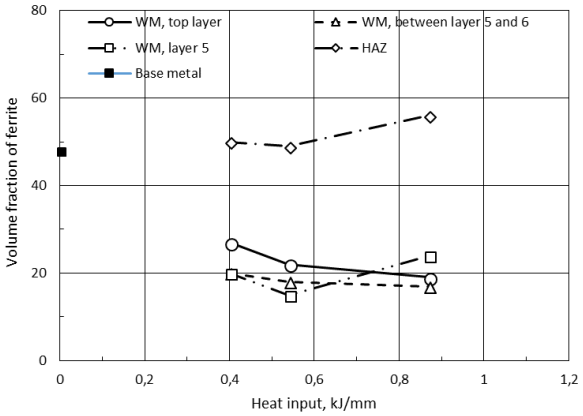

Fig.5. Effect of heat input on volume fraction of ferrite for different areas.

Precipitation of Cr nitrides was featured in the ferrite grain interiors in HAZ and occurs during cooling from temperatures in the range between 1250 to 1100°C, as shown in the micrograph in Fig.6b. The nitrides seem to concentrate inside the grains, with nitride free regions close to the austenite. Nitrides are liable to form during rapid cooling from high temperatures as ferrite is supersaturated with nitrogen [22-24].

When, this metastable microstructure is reheated above say 800°C, as the case in multipass welding and layer manufacturing, the most apparent change is the

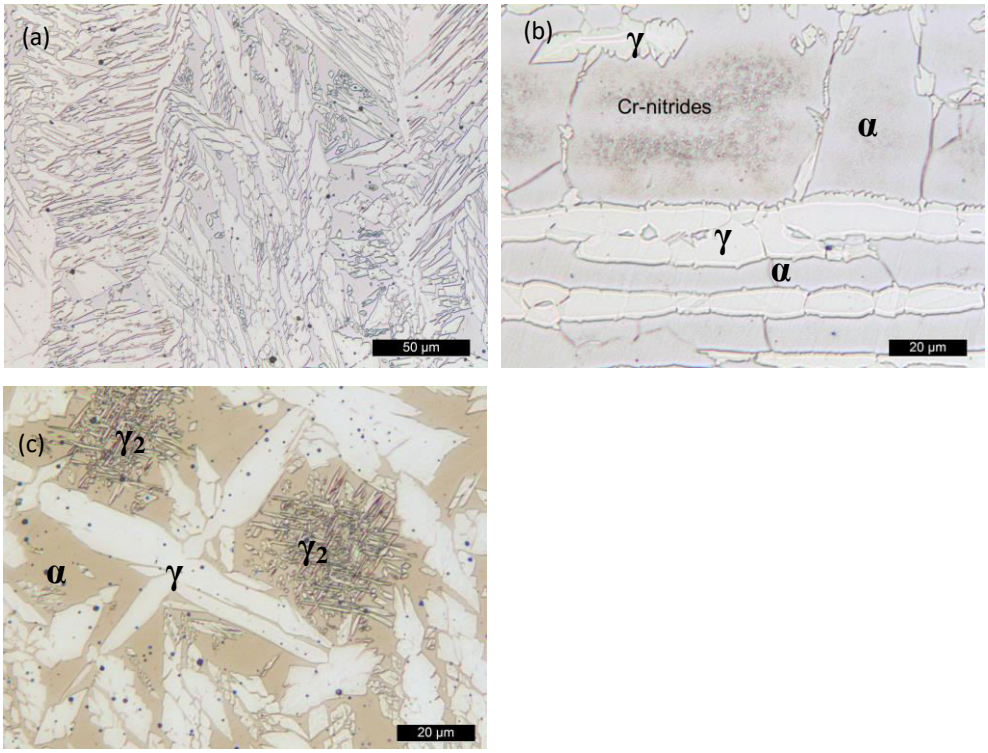

Fig.6. Microstructures. (a) Top layer (ferrite: grey, austenite: white), (b) Cr nitrides in ferrite in HAZ, and (c) secondary austenite in reheated ferrite.

precipitation of secondary austenite (γ_2) [25, 26]. The austenite precipitation may take place at γ/α interfaces [27], as well as intragranularly in the ferrite [28], the latter occurred most frequently in the present investigation, Fig.6c. Secondary austenite is reported to improve toughness [29] but may be harmful to corrosion [26]. Examination of corrosion properties will be the next step in the WAAM development of superduplex stainless steel.

Numerous types of intermetallic phases may form in superduplex stainless steels. The sigma phase which forms in the temperature range from 600 to 1000°C, has not been found with light microscopy using etchants that reveal σ. The formation of sigma is relatively sluggish because of the large tetragonal unit cell of 32 atoms [25]. However, alloying additions such as Cr, Mo and W accelerate the formation of σ by enlarging its field of stability. In wire arc additive manufacturing, building multilayers, care must be taken in heat input selection due to reheating by successive weld beads to avoid intermetallic phases due to their negative effect on toughness and corrosion.

4 Conclusions

Based on the present study, the following conclusions are drawn:

- No weld defects were found for any heat input.
- The yield and tensile strength levels were high, the yield strength approached or fell below that of the base metal for the highest heat input.
- The Charpy V notch toughness of the walls (~ 100J) at -20°C is only one third of the base metal.
- The ferrite volume fraction was only around 0.20 due to overalloying. This is more than 50% reduction compared with the base metal.

- Both Cr nitrides and secondary austenite were observed, while no intermetallic phases were found.
- The current WAAM process is fully applicable to superduplex stainless steel, where due care must be taken concerning welding and operational parameters, as well as component design to avoid formation of harmful secondary phases.

References

1. W. Frazier, J. Mater. Eng. Perform. **23**, 1917-1928 (2014)
2. D. Ding, Z. Pan, D. Cuiuri, H. Li, Int. J. Adv. Manu. Technol. **81**, 465–481 (2015)
3. I. Tolosa, F. Garciandía, F. Zubiri, F. Zapirain, A. Esnaola, Int. J. Adv. Manufac. Technol. **51**, 639-647 (2010)
4. E. Yasa, J-P. Kruth, Proc. Eng. **19**, 389-395 (2011)
5. M.S.F. Lima, S. Sankaré, Mater. Des. **55**, 526-532 (2014)
6. Z. Wang, T.A. Palmer, A.M. Beese, Acta Mater. **110**, 226-235 (2016)
7. M. Pohl, O. Storz, T. Glogowski, Mater. Charact. **58**, 65–71 (2007)
8. J.M. Pardal, S.S.M. Tavares, M. Cindra Fonseca, J.A. de Souza, R.R.A., Côrte, H.F.G. de Abreu, Mater. Charact. **60**, 165-172 (2009)
9. T.A. Palmer, J.T. Elmer, S.S. Babu, Mater. Sci. Eng. **374A**, 307-321 (2004)
10. T.G. Gooch, Proc. Int. Conf. *Duplex stainless steels'82*, ASM, St. Louis, USA, 573-602 (1983)
11. Z. Sun, M., Kuo, I.Y. Annergren, D. Pan,. Mater. Sci. Eng. **356A**, 274-282 (2003)
12. V. Muthupandi, P.B. Srinivasan, S.K. Seshadri, S. Sundaresan, Mater. Sci. Eng. **358A**, 9-16 (2003)
13. J. Yang, Q. Wang, Z. Wei, K. Guan, Case Studies in Eng. Fail. **A. 2**, 69-75 (2014)
14. J. Charles, Proc. Int. Conf. *Duplex Stainless Steels '91*, in: J. Charles, S. Bernhardsson (Eds.), Beaune, Les éditions de physique, 1991, pp. 3–48 (1991)
15. S. Pak, K. Karlsson, Scand. J. Metall. **19**, 9-13 (1990)
16. H. Kajimura, K. Ogawa, H. Nagano, ISIJ Int. **31**, 216-222 (1991)
17. K. Ogawa, Y. Komizo, S. Azuma, T. Kudo, Trans. Jpn. Weld. Soc. **23**, 40-45 (1992)
18. H. Kokawa, M. Tomita, T. Kuwana, Weld. Int. **9**, 8-15 (1995)
19. S. Hertzman, R. Jargelius Pettersson, R. Blom, E. Kivineva, J. Eriksson,. ISIJ Int. **36**, 968-976 (1996)
20. R. Mundt, H. Hoffmeister, Proc. Int. Conf. *Stainless Steels '84*, Gothenburg, The Metals Society, 315-322 (1985)
21. M. Liljas, Proc. Fourth Int. Conf. on *Duplex Stainless Steels*, Glasgow, Scotland, Keynote Paper V, vol. 2, 13–16 (1994)
22. R.F.A. Pettersson, S. Hertzman, S. Szakalos, P.J. Ferreira, Proc. Int. Conf. *Duplex Stainless Steels'94*, Glasgow, Scotland, 461–72 (1994)
23. J. Liao, ISIJ Int. **41**, 460–467 (2001)
24. T.H. Chen, J.R. Yang, Mater. Sci. Eng. **338A**, 166–81 (2002)
25. S. Atamert, J.E. King, Z. Metallkd. **82**, 230-239 (1991)
26. J.O. Nilsson, L. Karlsson, J.O. Andersson, L' Acciaio Inossidabile **1**, 18-22 (1994)
27. A.J. Ramírez, S.D. Brandi, J.C. Lippold, Acta Microscopica **10**, 147-148 (2001)
28. A.J. Ramirez, J.C. Lippold, S.D. Brandi, Metall. Mater. Trans. **34A**, 1575-1597 (2003)
29. J.C. Lippold A.M. Al-Rumaih, Proc. Int. Conf. *Duplex Stainless Steels '97*, KCI, Maastricht, The Netherlands, 1005-1010 (1997)